Available online at www.sciencedirect.com
SCIENCE DIRECT®
PERGAMON
International Journal of Heat and Mass Transfer 46 (2003) 2485–2493
International Journal of HEAT and MASS TRANSFER
www.elsevier.com/locate/ijhmt

Numerical simulation of the cooling of a hot disk rapidly subjected to combined convective and radiant heat losses

A. Ferriere [a,*], C. Chaussavoine [b], J.-P. Leyris [b], J. Hameury [c]

[a] CNRS-IMP, Centre du four solaire Felix Trombe, BP5, 66125 Odeillo, France
[b] CNRS-IMP, Université de Perpignan, 52 av. de Villeneuve, 66860 Perpignan, France
[c] LNE, 29 av. Roger Hennequin, 78197 Trappes, France

Received 13 January 2002

Abstract

The development of a transient method for measuring the spectral directional emissivity of solid materials at high temperature is currently being completed by the analysis of the influence of various sources of error. A hot disk is subjected to mixed convective and radiant heat losses on one face after the rapid withdrawal of a shutter. The cooling is investigated during a short period of observation through numerical simulations of the transient temperature. The thermal problem is simulated using 3D and axisymmetric 2D codes. The progressive withdrawal of the shutter results in a delay for the transient temperature in comparison with the instantaneous withdrawal. For an insulating material, the influence of the side wall boundary conditions remains negligible at the center of the front face. The strong influence of the convective heat transfer is demonstrated.

Keywords: Heat conduction; Transient thermal modeling; Numerical simulation; Emissivity measurement

1. Introduction

A method for measuring the spectral directional emissivity of solid materials at high temperature was developed by Redgrove [1,2]. It was implemented at the Laboratoire National d'Essais (LNE, France) by Morice [3]. It consists of measuring the radiance of the surface of a hot disk-shaped sample with a spectroradiometer and comparing the measured value with the radiance of the black body at the same temperature. The sample is heated in a closed furnace. The cap is opened, then a hot shutter is rapidly withdrawn to view the sample which starts to cool down. A sketch of the experimental set-up is given in Fig. 1. Current investigations aim to improve the accuracy and the reliability of the measurement technique to make it a viable technique to provide reference values of emissivity factors in the range 350–1200 K. The determination of the emissivity is based on the reconstruction of the transient temperature of the central area of the front face of the disk-shaped sample, which is viewed by the spectroradiometer, during the very beginning of the cooling. The current method uses a 1-D computer code to simulate the transient temperature. Major simplifying assumptions are made. The temperature is assumed to be uniform on the front face. The protective shutter is assumed to be instantaneously withdrawn. We assume that the convective heat loss is represented by a constant heat transfer coefficient that is roughly estimated. The strategy for improving the method relies on the utilization of high performance computer codes to simulate 2-D and 3-D conduction heat transfers with a fine time and space resolution. The aim of this work is to identify the most influential

* Corresponding author. Tel.: +33-4-68-30-77-49; fax: +33-4-68-30-29-40.
E-mail address: alain.ferriere@imp.cnrs.fr (A. Ferriere).

0017-9310/03/$ - see front matter
doi:10.1016/S0017-9310(02)00548-3

Nomenclature

T	temperature, function of space and time (K)
T_0	initial uniform temperature (K)
T_∞	ambient temperature (K)
X	space variable, $X = (x, y, z)$ in Cartesian coordinates for example
t	time variable (s)
$\dot{q}_{\text{conv}}$	convective heat loss (W/m^2)
h	heat transfer coefficient (W/m^2 K)
ε	total hemispherical emissivity factor of the sample
ε_{sh}	total hemispherical emissivity factor of the shutter
$\dot{q}_{\text{rad}}$	radiant heat loss (W/m^2)
$F_{dS\to\text{sh}}$	configuration factor from an elemental area dS to the shutter
R_{sh}	radius of the shutter (60 mm)
e	thickness of the shutter (10 mm)
D	distance between the plane of the front face and the plane of the shutter (5 mm)
d	distance between the axis of the sample and the axis of the shutter

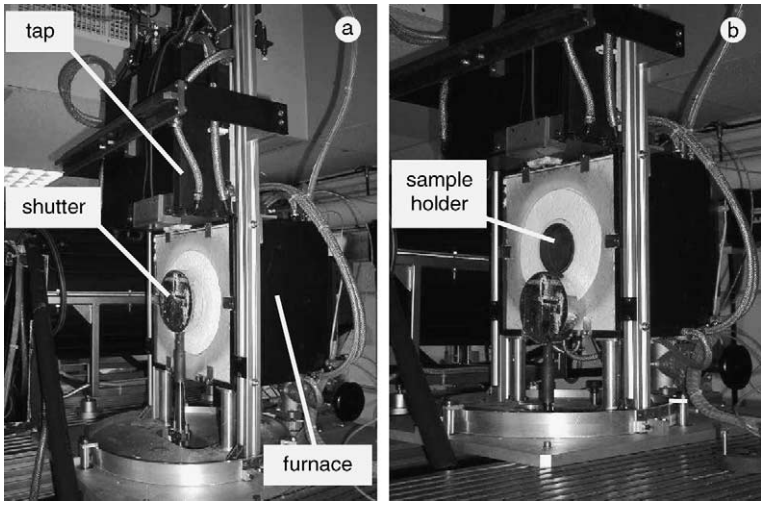

Fig. 1. (a) Picture of the furnace with the tap opened and the shutter closed. (b) Picture of the furnace with the tap opened and the shutter withdrawn.

parameters that affect the temperature and consequently the radiative signal during the beginning of the cooling. The investigations reported in this paper consider the effects of the side wall boundary conditions, of the progressive withdrawal of the shutter, and of the time dependence of the convective heat loss on the distribution and on the transient evolution of the temperature on the front face. We consider the initial period of cooling up to 500 ms, with consequently small variations of temperature (maximum 10 K).

2. Thermal problem

The transient temperature of the front face of the sample is simulated for 50, 100, 200 and 500 ms, with a time step of 0.5, 1, 2 and 5 ms, respectively. The sample is a disk 5 mm in thickness and 20 mm in diameter, made of homogeneous and isotropic material. Four materials are selected, in order to cover a large range of thermophysical properties: steel, zirconia, silica, and silica coated with a thin film of gold on the front face. The thermophysical properties of these materials are indicated in Table 1. The heat conduction problem is classically governed by the following system:

$$\rho C_{\text{p}} \frac{\partial T}{\partial t} = \lambda \Delta T \tag{1}$$

The boundary conditions considered on the side wall and on the rear face of the sample are identical. Practically, only the side wall is influential on the evolution of the front face temperature, because of the short time simulated. Three types of boundary conditions are considered:

Table 1
Thermophysical properties of steel, silica, silica coated with gold, and zirconia at 800 K (source: LNE-BNM)

	Thermal conductivity (W/m K)	Heat capacity (J/kg K)	Density (kg/m^3)	Total hemispherical emissivity
Steel	45	500	7800	0.7
Silica	2	1050	2200	0.95
Silica coated with gold	2	1050	2200	0.05
Zirconia	2	680	5600	0.6

- Contact thermal resistance R_{tc} between the sample and the body of the furnace assumed to remain at the steady state temperature T_0:

$$-\lambda\left[\frac{\partial T(X,t)}{\partial \vec{n}}\right]_{\text{rear+side}} = \frac{T(X,t)-T_0}{R_{tc}} \tag{2}$$

  This contact thermal resistance is roughly estimated between 0.04 and 0.004 m^2 K/W.
- Perfect contact with the body of the furnace at T_0:

$$[T(X,t)]_{\text{rear+side}} = T_0 \tag{3}$$

- Perfect insulation of the sample:

$$\left[\frac{\partial T(X,t)}{\partial \vec{n}}\right]_{\text{rear+side}} = 0 \tag{4}$$

Eqs. (3) and (4) are the cases, non-realistic but commonly used as simplified models, where R_{tc} tends respectively to 0 and to $+\infty$.

The boundary condition on the front face of the sample represents combined convective and radiant heat losses, which depend on the progressive withdrawal of the shutter:

$$-\lambda\left[\frac{\partial T(X,t)}{\partial \vec{n}}\right]_{\text{front}} = \dot{q}_{\text{conv}}(X,t) + \dot{q}_{\text{rad}}(X,t) \tag{5}$$

The initial temperature is assumed to be uniform in the whole sample: $T_0 = 800$ K.

2.1. Convective heat loss

Both natural and forced convective heat transfer take place, due to the vertical orientation of the front face and the movement of the shutter. Assuming that the diameter of the sample is negligible in comparison with the scale of the movements of fluid, the convective heat loss is expressed using a time-dependent heat transfer coefficient $h(t)$:

$$\dot{q}_{\text{conv}}(X,t) = h(t)[T(X,t) - T_\infty] \tag{6}$$

Using classical correlation for a vertical flat plate given by Taine and Petit [4], peak values of $h(t)$ are roughly estimated in three cases:

1. Internal natural convection, in the presence of the shutter: $h_1 = 3$ W/m^2 K.
2. Forced external convection, during the movement of the shutter: $h_2 = 20$ W/m^2 K.
3. External natural convection, after the shutter is withdrawn: $h_3 = 10$ W/m^2 K.

The model of $h(t)$ plotted in Fig. 2 has no real physical meaning other than simply fitting with the three values estimated above.

2.2. Configuration factor between an elemental surface of the sample and the shutter

The sketch in Fig. 1 shows the positions of the sample and of the shutter during the withdrawal. Let d be the

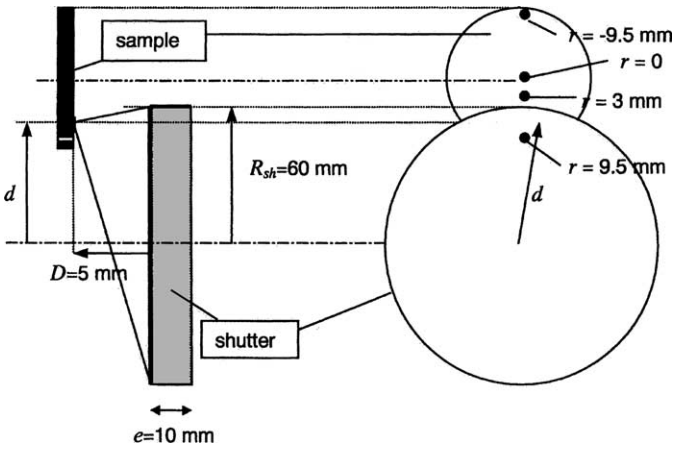

Fig. 2. Sketch of the experimental set-up: sample and shutter orientations side (left) and front (right) views.

distance between the center of the shutter and the projection of the point X on the shutter. The configuration factor $F_{dS\to sh}$ between an elemental area dS centered on the point X and the shutter depends on the distance d.

2.2.1. The normal to the area dS intercepts the shutter

The configuration factor is given by Siegel and Howell [5]:

$$\text{For } d=0: \quad F_{dS\to sh}=\frac{R_{sh}^2}{D^2+R_{sh}^2} \tag{7}$$

$$\text{For } 0<d<R_{sh}: \quad F_{dS\to sh}=\frac{1}{2}\left\{1-\frac{1+\Delta^2-\Omega^2}{\sqrt{\Gamma^2-4\Omega^2}}\right\} \tag{8}$$

With $\Delta=\frac{D}{d}$, $\Omega=\frac{R_{sh}}{d}$, $\Gamma=1+\Delta^2+\Omega^2$

2.2.2. The normal to the area dS does not intercept the shutter

Here $d \geqslant R_{sh}$, and there is no analytical expression for the configuration factor between the element dS and the cylindrical edge of the shutter. We have calculated it by combining configuration factors between cylinders. We propose a polynomial expression for $F_{dS\to sh}$:

$$F_{dS\to sh}=\sum_{i=0}^{10}\alpha_i d^i \tag{9}$$

In the experimental set-up, the distance D between the sample and the shutter equals 5 mm, the radius R_{sh} of the shutter equals 60 mm, and the thickness of the shutter equals 10 mm. The values of the coefficients α_i are given in Table 2. The great number of significant digits is required to prevent any numerical divergence when computing the values of $F_{dS\to sh}$.

2.2.3. Evolution of the configuration factor $F_{dS\to sh}$

During the withdrawal of the shutter, this configuration factor decreases from 1 to 0, according to the velocity of the movement and to the position of the point considered on the front face of the sample. The average velocity of the withdrawal was measured. It equals 5.417 m/s. To illustrate the variation of $F_{dS\to sh}$, four relevant points are considered.

- the center of the sample ($r=0$)
- the point at the limit of the area viewed by the radiometer ($r=3$ mm)
- two points located at the top and at the bottom of the front face ($r=-9.5$ and 9.5 mm, respectively).

Table 2
Coefficients of the polynomial expression of the configuration factor $F_{dS\to sh}$

Coefficient	Value
α_0	927.67539839
α_1	−76.471820648
α_2	2.6680190316
α_3	$-4.9674315754\times10^{-2}$
α_4	$4.8536606229\times10^{-4}$
α_5	-1.22023551×10^{-6}
α_6	$-2.7275916989\times10^{-8}$
α_7	$3.5956291609\times10^{-10}$
α_8	$-2.0568360453\times10^{-12}$
α_9	$5.9905506653\times10^{-15}$
α_{10}	$-7.231622478\times10^{-18}$

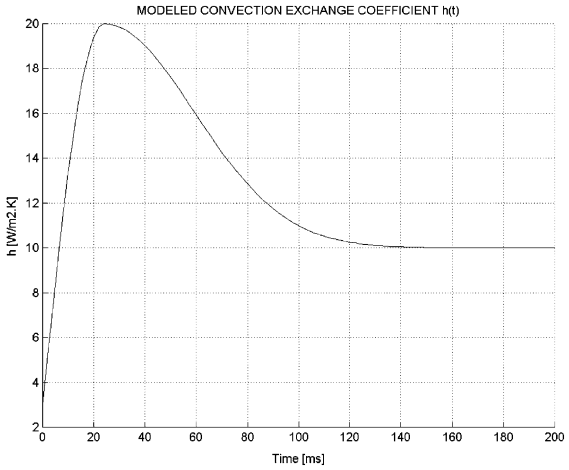

Fig. 3. Transient convective heat transfer coefficient (modeled).

The evolutions of $F_{dS\to sh}$ are plotted on Fig. 3. A time-lag of about 3.5 ms is observed between the evolutions of the configuration factors of two points located respectively at $r=-9.5$ and 9.5 mm. This result is consistent with the velocity of the movement.

2.3. Radiant heat loss

The radiant heat loss is the difference between the radiosity $\dot{q}_o$ of the the sample and the incident energy on the sample $\dot{q}_i$:

$$\dot{q}_{rad}=\dot{q}_o-\dot{q}_i \tag{10}$$

The radiosity is composed by the emitted plus the reflected energy:

$$\dot{q}_o=\varepsilon_S\sigma T_S^4+\rho_S\dot{q}_i \tag{11}$$

The incident energy is composed by the flux coming from the shutter plus the flux coming from the infinite medium:

$$\dot{q}_i=F_{dS\to sh}\ \dot{q}_{o,sh}+F_{dS\to\infty}\ \dot{q}_{o,\infty} \tag{12}$$

The configuration factors are additive, so:

$$F_{dS\to\infty}+F_{dS\to sh}=1 \tag{13}$$

The radiosity from the shutter is:

$$\dot{q}_{o,sh} = \varepsilon_{sh}\sigma T_{sh}^4 + \rho_{sh}\dot{q}_{i,sh} \quad (14)$$

And the contribution from the infinite medium is:

$$\dot{q}_{o,\infty} = \sigma T_{\infty}^4 \quad (15)$$

We assume that the surfaces of the sample and of the shutter are grey, opaque, and perfectly diffusive. We also assume that the incident energy on the shutter $\dot{q}_{i,sh}$ only comes from the infinite medium at T_∞:

$$\dot{q}_{i,sh} = \sigma T_{\infty}^4 \quad (16)$$

Hence it comes from Eqs. (10)–(16) the following expression of the radiant heat loss as a function of time for every point of the front face:

$$\dot{q}_{rad}(X,t) = \varepsilon\sigma\{T(X,t)^4 - T_{\infty}^4 - F_{dS\to sh}(X,t)\varepsilon_{sh}(T_0^4 - T_{\infty}^4)\} \quad (17)$$

3. Discussion

3.1. Effect of the movement of the shutter

In the case of perfect insulation of the side wall and only radiant heat loss on the front face, the cooling of a zirconia sample is simulated using the 3-D simulation code for a period of 50 ms, twice as long as the withdrawal of the shutter. The transient temperature of the four points located at $r = 0$, 3, 9.5, −9.5 mm on the front face is computed and plotted in Fig. 4, using two values for the total hemispherical emissivity factor of the shutter: $\varepsilon_{sh} = 0.5$ and 0.8. No significant difference is observed between the cooling curves of the four points. The 3-D effect resulting from the progressive withdrawal of the shutter is thus found to be negligible. However, the value of the emissivity of the shutter strongly influences the cooling rate: a high emissivity of the shutter counterbalances the radiant heat loss of the sample. The influence of the movement of the shutter is then completely analyzed through the cooling curves of the center simulated with the axisymmetric 2-D code for 100 ms and assuming that the configuration factor of every point of the front face is equivalent to that of the central point. For this investigation we assume that side and rear walls are perfectly insulated in order to avoid additional influence of boundary conditions. For the first calculation, no convection is applied on the front face. The cooling curves of the center of a steel sample computed in two situations -progressive and instantaneous withdrawal of the shutter, are plotted on Fig. 5a, showing a time-lag between the two curves. This time-lag is also time dependent, but it stabilizes after the shutter is withdrawn. A complete investigation made with steel, silica and silica + gold and with various values of the emissivity factor of the shutter shows that this time-lag does not depend on the thermophysical

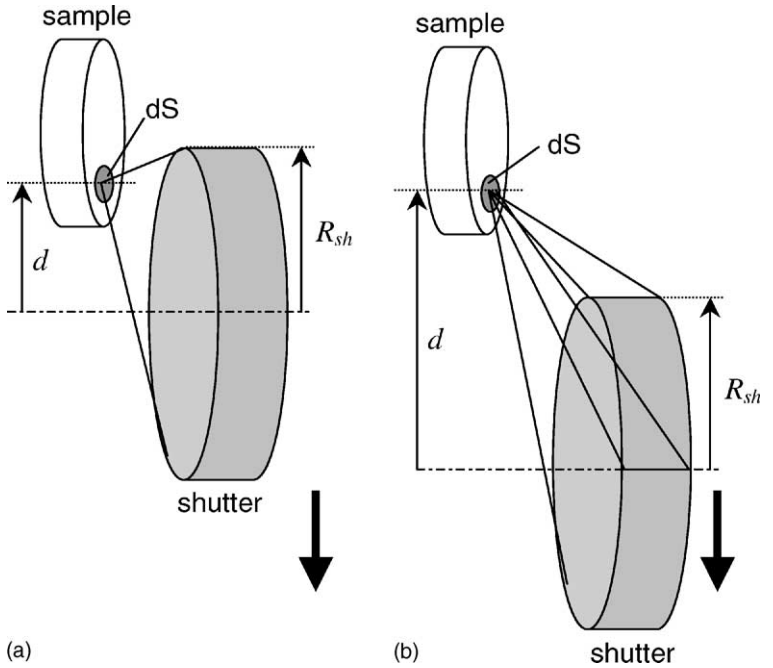

Fig. 4. (a) Sketch of the position of the shutter at the beginning of the withdrawal. (b) Sketch of the position of the shutter at the end of the withdrawal.

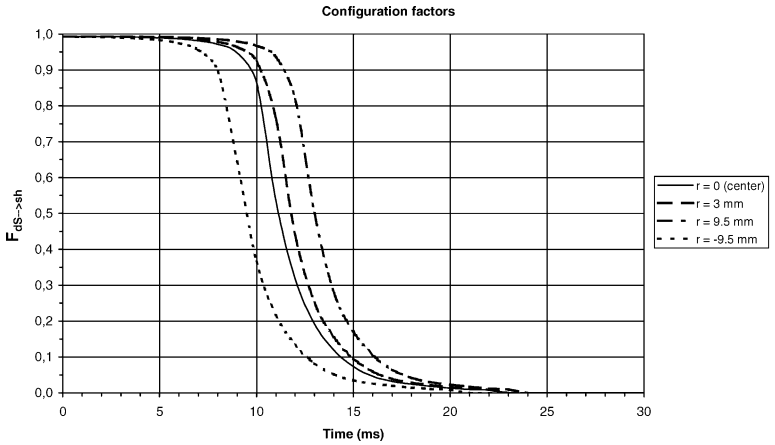

Fig. 5. Variation of the configuration factor $F_{dS\rightarrow sh}$ versus time. In four points located at $r = 0$, 3, 9.5 and -9.5 mm on the front face.

properties of the sample but it increases when the emissivity factor of the shutter increases. The time-lag stabilizes at 7.51, 8.98, and 11.88 ms when ε_{sh} equals 0.5, 0.6, and 0.8, respectively (see Fig. 5b).

For the second calculation, a constant and uniform convective heat exchange coefficient of 10 W/m^2 K is imposed at the front face. A faster cooling rate is observed (see Fig. 6a), and the time-lag stabilizes at lower values: 5.72, 6.84, and 9.07 ms when ε_{sh} equals 0.5, 0.6, and 0.8 respectively (see Fig. 6b).

In conclusion, the cooling curve strongly depends on the rate of the withdrawal of the shutter, on the emissivity of the shutter, and on the convective heat transfer coefficient. The time-lag between the cooling curves given by the instantaneous withdrawal and progressive withdrawal cannot be simply modeled as a function of the properties of the shutter. Thus the convective heat loss must be determined to correctly predict the cooling.

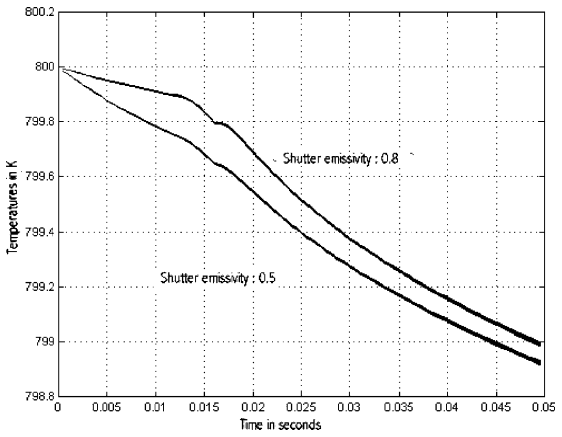

Fig. 6. Cooling curves of four points widely distributed on the front face ($r = 0$, 3, 9.5 and -9.5 mm). Zirconia sample, 3-D computing code, two values are considered for the emissivity factor of the shutter: $\varepsilon_{sh} = 0.5$ and 0.8.

3.2. Effect of the boundary conditions at the side wall

When the side wall is not perfectly insulated, the cooling of the front face of the sample is not uniform: the center cools down faster than the edges. This effect is investigated through the observation of the diameter of a quasi-isothermal area, defined as the area over which the amplitude of temperature remains lower than a given limit, typically 10^{-3}–10^{-2} K. Two materials are compared: one highly conductive—steel, and one highly insulating—silica. The radius of the sample is 10 mm in both cases. A period of 500 ms of cooling is simulated using the axisymmetric 2-D computer code. Both radiant and convective heat losses are simulated using constant coefficients. Two boundary conditions on the rear and side walls are simulated and compared: walls maintained at 800 K, and contact thermal resistance $R_{tc} = 0.004$ m^2 K/W between the walls and the body of the furnace at 800 K. This value of R_{tc} is the estimated low limit. The radius of the quasi-isothermal area at 10^{-3} K for the steel and the silica samples are plotted versus time in Fig. 7a. Note that the wavelets on the curves are caused by the linear interpolation made on the radius to determine the position of the points at the upper limit of temperature (edge of the quasi-isothermal area).

For the silica sample, the 10^{-3} K quasi-isothermal area slowly decreases. After 300 ms of cooling, the radius decreases from 10 to 7.5 mm when the walls are maintained at 800 K, and from 10 to 8.5 mm when the thermal contact resistance of 0.004 m^2 K/W is applied. This shows that the temperature of the central area of the front face of an insulating material is expected to remain uniform, and can thus be predicted using a 1D simulation code.

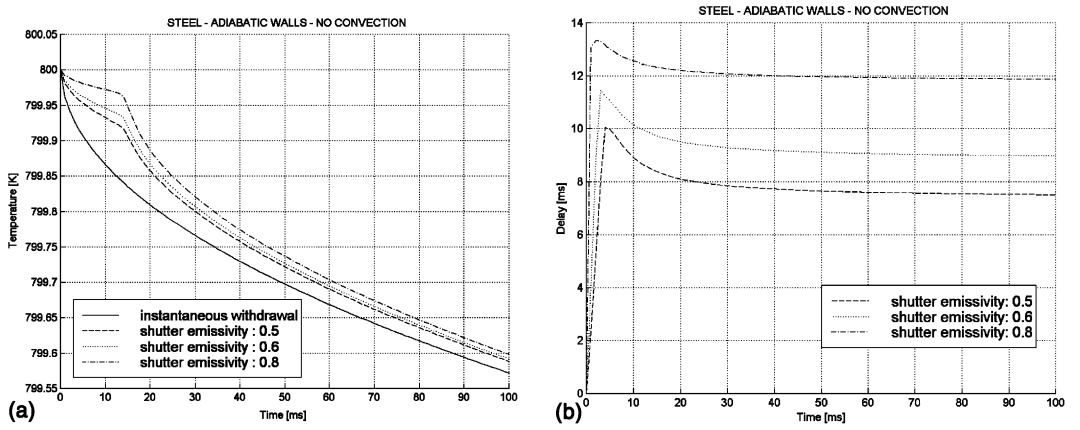

Fig. 7. (a) Cooling curves of the center of a steel sample 2-D computing code, instantaneous withdrawal and progressive withdrawal with ε_{sh} equal to 0.5, 0.6, and 0.8. No convection. (b) Time-lag between the cooling curves of the center of a steel sample. 2-D computing code, progressive withdrawal of the shutter, no convection.

For the steel sample, the quasi-isothermal area quickly decreases when the walls are maintained at 800 K, and the effect of thermal contact resistance is noticeable. After 300 ms of cooling, the radius of the 10^{-3} K quasi-isothermal area decreases to 2.5 mm and to 8 mm in each case respectively. The influence of the difference of temperature is investigated for the case of a steel sample with walls maintained at 800 K. The relevant changes of the radius of the quasi-isothermal areas are plotted in Fig. 7b. For a 10^{-2} K quasi-isothermal area, the radius decreases more slowly, reaching 4.7 mm after 300 ms. We conclude that an insulation or at least a thermal contact resistance on the side wall is recommended when working with a highly conductive material. The temperature of the central area is expected to remain uniform, and can be predicted using a 1-D simulation code. The measurement of the radiation emitted by this central area is meaningful for a duration of 500 ms. An alternative solution is to extend the diameter of the sample, but we did not explore it.

3.3. Effect of the convective heat loss

Three materials are compared: one highly conductive—steel, and two highly insulating—silica and silica coated with gold. In the last case, the gold layer makes the emissivity factor drop down to 0.05, and thus enhances the effect of convection in the mixed convective and radiant losses. The cooling of the center of the front face is simulated using the axisymmetric 2-D code for

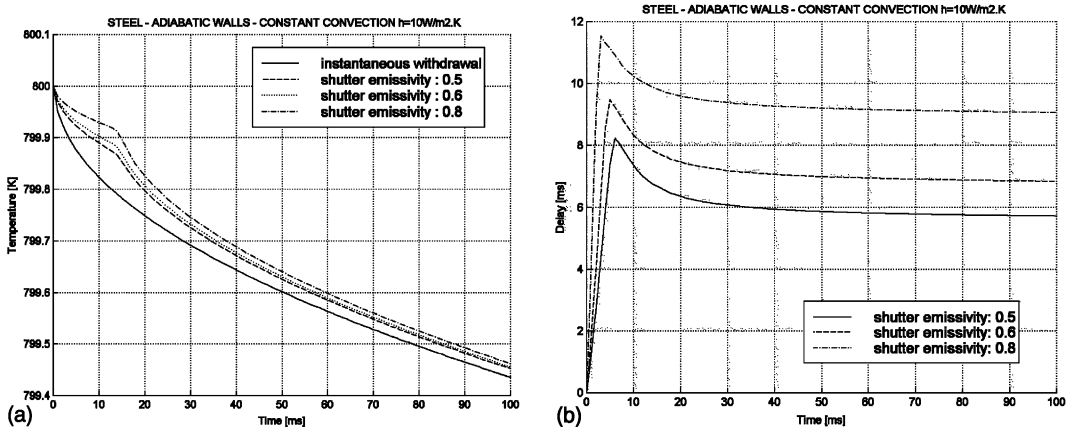

Fig. 8. (a) Cooling curves of the center of a steel sample 2-D computing code, instantaneous withdrawal and progressive withdrawal with ε_{sh} equal to 0.5, 0.6, and 0.8. Convection heat transfer coefficient $h = 10$ W/m^2 K. (b) Time-lag between the cooling curves of the center of a steel sample 2-D computing code, progressive withdrawal of the shutter. Convection heat transfer coefficient: $h = 10$ W/m^2 K.

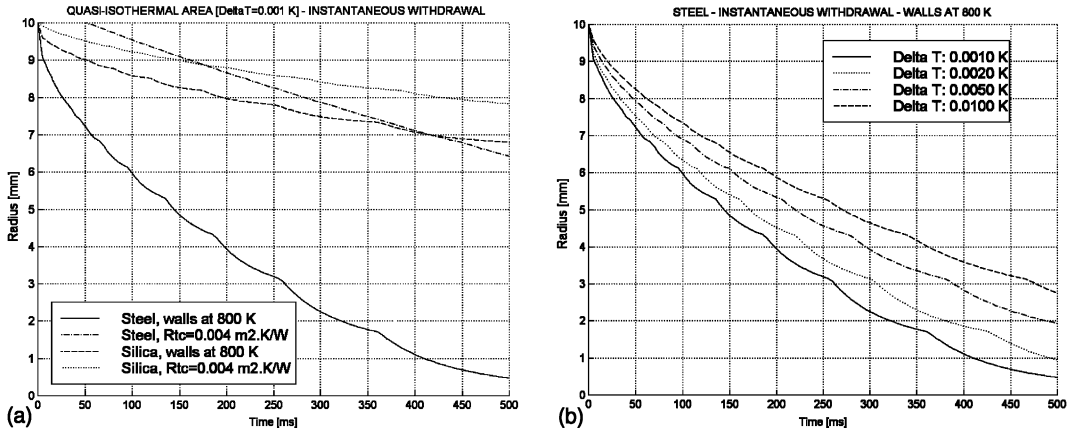

Fig. 9. (a) Quasi-isothermal area versus time $\Delta T = 10^{-3}$ K steel and silica samples, walls maintained at 800 K and thermal contact resistance. (b) Quasi-isothermal areas versus time $\Delta T = 10^{-3}, 2 \times 10^{-3}, 5 \times 10^{-3}, 10^{-2}$ K steel sample, side and rear walls maintained at 800 K.

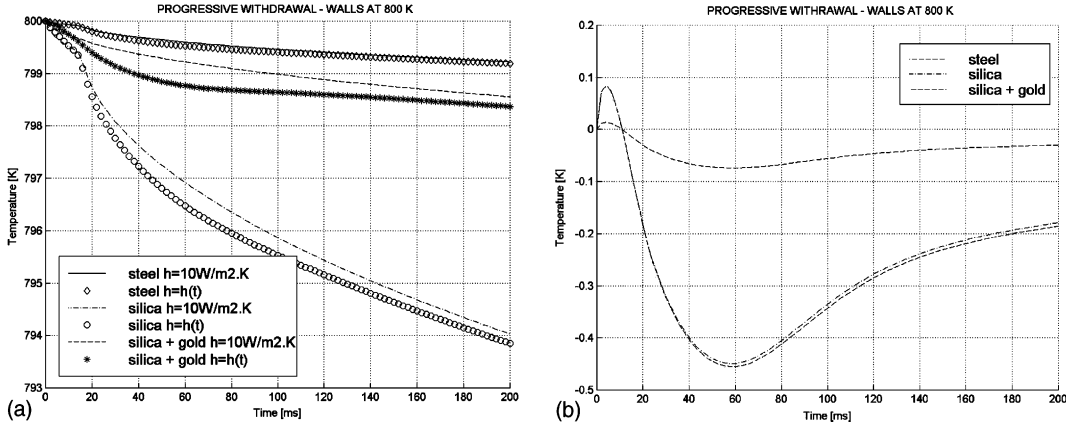

Fig. 10. (a) Transient temperature at the center, with $h = h(t)$ and with $h = 10$ W/m^2 K steel, silica, and silica coated with gold. (b) Deviation between transient temperatures with $h = h(t)$ and with $h = 10$ W/m^2 K steel, silica, and silica coated with gold.

200 ms, with a perfect contact ($T = 800$ K) and with adiabatic walls. For both materials, identical results are obtained at the center with adiabatic walls and with walls at 800 K. The transient heat transfer coefficient $h(t)$ as modeled in Section 2.1 (see Fig. 1) and the transient radiant heat loss as modeled in Section 2.3 (see Eq. (17)) are considered. The emissivity of the shutter is $\varepsilon_{sh} = 0.8$. The case of a constant heat transfer coefficient equal to the final value $h = 10$ W/m^2 K is also included in our simulations. We determine the effect of the progressive withdrawal of the shutter. The cooling curves are plotted in Fig. 8a, showing that the convective heat loss has a significant effect on the cooling of all materials. We also estimate the influence of the variation of the convection coefficient, through the comparison between the cooling curves at the center for the two cases $h = h(t)$ and $h =$ constant (see Fig. 8b). This influence is much greater in the case of both insulating materials, but no significant deviation is observed between a highly emissive (silica) and a poorly emissive material (silica + gold) (Fig. 9 and Fig. 10).

4. Conclusion

The thermal problem of the cooling of a hot disk subjected to mixed convective and radiant heat losses on one face after the rapid withdrawal of a shutter was investigated by simulating the transient temperature distribution with 3-D, axisymmetric 2-D, and 1-D computer codes. It was established that 3-D effects caused by the progressive withdrawal of the shutter remained negligible when the velocity of this movement is high—typically 25 ms for a complete withdrawal of 120

mm. The realistic case was simulated using the 2-D axisymmetric code, considering that the configuration factor for every point on the front face could be given by the value at the center. The progressive withdrawal of the shutter resulted in a time-lag for the transient temperature compared to the case of instantaneous withdrawal. The 2-D effects resulted only from the boundary conditions at the side wall. For short duration of observation—typically 500 ms, their influence remained negligible at the center of the front face when the thermal conductivity was low. In the experimental determination of the spectral directional emissivity factor of insulating materials at high temperature, the 1-D computer code can be successfully used for the reconstruction of the transient temperature of the central area of the sample at the very beginning of the cooling. For conductive materials, the axisymmetric 2-D model must be used. More generally, the signal measured by the radiometer cannot be simply extrapolated to obtain the initial value at $t = 0$. A careful determination of the convective heat loss must be done before we can predict the early cooling with enough accuracy to significantly improve the method of measurement of the emissivity. The convective heat transfer coefficient is assumed to be uniform, but the time distribution must be carefully determined. Accurate estimation of the emissivity factor of the shutter is also required, since our model showed that it strongly influences the cooling curve.

Acknowledgements

The authors are grateful to the Bureau National de Metrologie, who supported this work with contract # 98 4 002.

References

[1] J.S. Redgrove, A new method for accurate measurement of spectral emissivity, High Temp.—High Press. 17 (1985) 145–151.
[2] J.S. Redgrove, Measurement of the spectral emissivity of solid materials, Measurement 8 (2) (1990) 90–95.
[3] R. Morice, Développement d'une installation pour la mesure en régime transitoire de l'émissivité spectrale directionnelle des matériaux à haute température, Ed. CNAM Paris (France), Energétique, Machines et Moteurs, February 1998.
[4] J. Taine, J.-P. Petit, in: Transferts Thermiques, Mécanique des Fluides Anisothermes, second ed., Ed. Dunod, Paris (France), 1998.
[5] R. Siegel, J.R. Howell, Thermal Radiation Heat Transfer, third ed., Ed. Taylor and Francis, 1992.